

ChemComm

Chemical Communications

Accepted Manuscript

This article can be cited before page numbers have been issued, to do this please use: X. Zhuang, X. Gao, C. Tian, D. Cui, F. Luan, Z. wang, Y. Xiong and L. Chen, *Chem. Commun.*, 2020, DOI: 10.1039/D0CC01573C.



This is an Accepted Manuscript, which has been through the Royal Society of Chemistry peer review process and has been accepted for publication.

Accepted Manuscripts are published online shortly after acceptance, before technical editing, formatting and proof reading. Using this free service, authors can make their results available to the community, in citable form, before we publish the edited article. We will replace this Accepted Manuscript with the edited and formatted Advance Article as soon as it is available.

You can find more information about Accepted Manuscripts in the [Information for Authors](#).

Please note that technical editing may introduce minor changes to the text and/or graphics, which may alter content. The journal's standard [Terms & Conditions](#) and the [Ethical guidelines](#) still apply. In no event shall the Royal Society of Chemistry be held responsible for any errors or omissions in this Accepted Manuscript or any consequences arising from the use of any information it contains.

COMMUNICATION

Synthesis of europium(III)-doped copper nanoclusters for electrochemiluminescence bioanalysis

Received 00th January 20xx,
Accepted 00th January 20xx

Xuming Zhuang^{a,b}, Xueqing Gao^b, Chunyuan Tian^b, Deliang Cui^a, Feng Luan^b, Zhenguang Wang^{d,*},
Yuan Xiong^e, Lingxin Chen^{c,*}

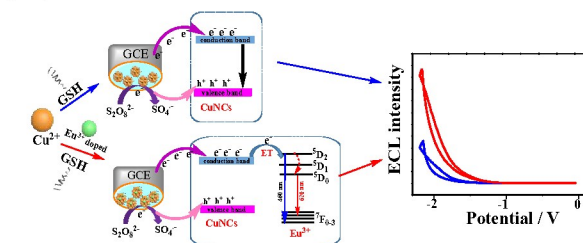
DOI: 10.1039/x0xx00000x

An electrochemiluminescence biosensor based on europium (III)-doped copper nanoclusters was proposed for the first time to achieve rapid and sensitive bioanalysis, using dopamine detection as a model.

Nanomaterial-based electrochemiluminescence (ECL) has emerged as a promising analytical technique in the developing of analytical sensors, due to its high sensitivity, wide dynamic range and low background, based on the variable optical, electronic and electrochemical properties of nanomaterials.¹ In particular semiconductor nanocrystals, such as CdS,² PbS,³ CdSe,⁴ CuInS,⁵ and lead halide perovskites⁶ have been reported as emitters of ECL, and showed advantages of high photoluminescence (PL) quantum yield (QY), high photostability, and narrow emission bands. Unfortunately, many of these NCs contain toxic heavy metals (Cd or Pb), which raises serious environmental and health concerns. Especially for bioanalysis, ECL emitters which are non/low-toxic and environmentally friendly are strongly preferred.

Metal nanoclusters (NCs), which are made up of a few-nm metal core surrounded by organic ligands, is yet another kind of rather efficient light-emitting nanoparticles, with additional advantages of bio-compatibility or at least low toxicity.⁷ Au and Ag based NCs have been developed as ECL emitters, and already used for chemical sensing and bioanalysis.^{8,9} Peng and co-workers used ECL sensing platform based on high-quantum-yield Au NCs probe for glutathione

detection; Zhou and co-workers designed an ECL biosensor for the detection of Cyclin-D1 by utilizing in situ electrogenerated Ag NCs. Being in the same group as Au and Ag in the periodic table of elements, CuNCs may also offer ECL properties.¹⁰ In addition, Cu is cheap, earth-abundant element, which is also an essential trace element in a human body.¹¹ This gives Cu additional advantages in sensing, as compared to Au and Ag. However, compared with the extensively studied Au and Ag NCs, ECL related applications of CuNCs in analytical sensing are lagged behind, due to the ease of the oxidation of copper, and rather weak ECL signals. Zhao and co-workers reported the feasibility of using bovine serum albumin protected CuNCs as an emitter, which was combine with hydrazine as a co-reactant, and then used for dopamine (DA) detection.¹² Here, we proposed the rare-earth element doping strategy with Eu(III) to improve the stability of CuNCs and to increase their ECL intensity, utilizing the rich electronic structure of the rare earth element, which could provide the remarkable optical properties.



Scheme 1. Comparison of ECL mechanisms of CuNCs and Eu³⁺-CuNCs.

An ECL biosensor based on Eu³⁺ ion doped CuNCs was fabricated for bioanalysis, taking the detection of DA as a model system. DA is an important catecholamine neurotransmitter, which plays an important role in cognition, emotion, memory, exercise and endocrine function in humans. Abnormal levels of DA in living organisms can lead to a series of diseases and even life-threatening conditions, such as Parkinson's disease, schizophrenia and ADHD.¹³ Therefore, sensitive and accurate detection of DA is highly desired for clinical diagnosis.^{14,15}

^aState Key Laboratory of Crystal Materials, Shandong University, Jinan 250100, China.

^bCollege of Chemistry and Chemical Engineering, Yantai University, Yantai 264005, China.

^cCAS Key Laboratory of Coastal Environmental Processes and Ecological Remediation, Shandong Key Laboratory of Coastal Environmental Processes, Yantai Institute of Coastal Zone Research, Chinese Academy of Sciences, Yantai 264003, China. E-mail address: lxchen@yic.ac.cn (L. Chen).

^dCollege of Chemistry and Environmental Science, Hebei University, Baoding 071002, China. E-mail address: wzg583@163.com (Z. Wang).

^eShenzhen Research Institute, City University of Hong Kong, Shenzhen, 518057, China.

*Corresponding author.

Electronic Supplementary Information (ESI) available: [details of any supplementary information available should be included here]. See DOI: 10.1039/x0xx00000x

As shown in Scheme 1, the Eu(III)-doped CuNCs (Eu³⁺-CuNCs) were synthesized from Cu²⁺ by using glutathione as both reducing agent and stabilizer,¹⁶ in the presence of Eu(III) salt. The transmission electron microscopy (TEM) image (Fig. 1A) suggests the formation of well dispersed Eu³⁺-CuNCs, with an average size approximate 5 nm. The presence of the poly(vinylpyrrolidone) makes it difficult to achieve high TEM image contrast, energy dispersive spectrometry (EDS) (Fig. 1B) combined with elemental mapping (Fig. 1C-E) was performed to prove the presence of Eu³⁺ ion in CuNCs. The well-matched color of Cu (Fig. 1D) and Eu (Fig. 1E) elements with the HAADF TEM image taken from the same sample area confirm the homogeneous distribution of Eu³⁺ ion throughout the CuNCs structure.

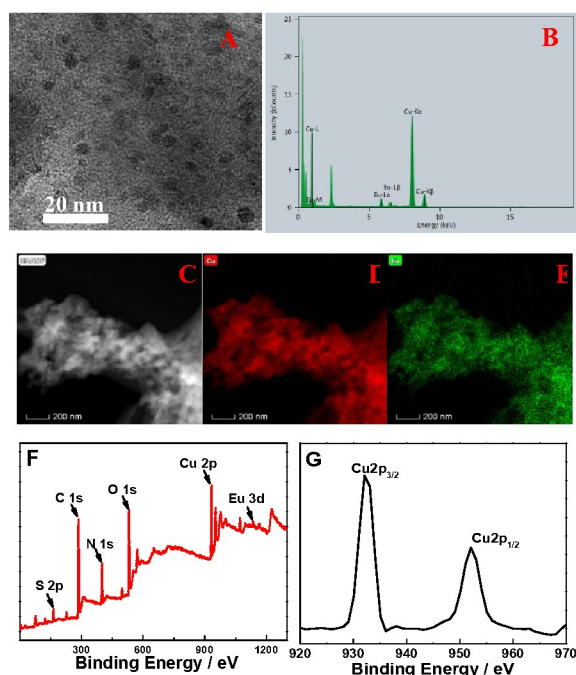


Fig. 1. Characterization of Eu³⁺-CuNCs: (A) TEM image; (B) EDS analysis. (C) HAADF TEM image; Elemental mapping of Cu (D) and Eu (E); (F) XPS survey spectrum; (G) Expanded XPS spectrum of Cu 2p.

X-ray photoelectron spectroscopy (XPS) has been further used to determine the composition of the Eu³⁺-CuNCs. The survey XPS spectrum in Fig. 1F confirms the presence of all the expected elements, including C, N, O, S, Cu, and Eu. Moreover, the Cu 2p electron spectrum (Fig. 1G) showed that the peaks at 932.4 and 952.5 eV were attributed to Cu2p_{3/2} and Cu2p_{1/2} of Cu(0), respectively, and there was no satellite peak at 943.7 eV, indicating that Cu(II) was almost absent in the system. The state of Cu(I) differs from the 2p_{3/2} binding energy of Cu (0) only by approximately 0.1 eV; therefore, the valence state between 0 and +1 is most likely for this element.¹⁷ The peak at 1134.9 eV was attributed to Eu 3d (Fig. S1), which is consistent with the reported literature.¹⁸ FT-IR spectra shown in Fig. S2 have similar peaks for Eu³⁺-CuNCs and bare pure CuNCs,

pointing out that the doped Eu³⁺ ion have little effect on the characteristic functional groups of CuNCs.

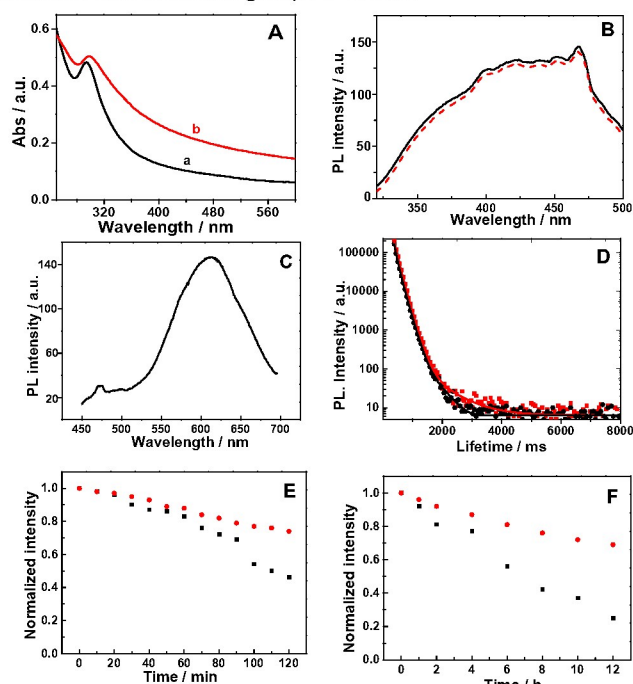


Fig. 2. (A) UV-vis spectra of CuNCs (a) and Eu³⁺-CuNCs (b). (B) PLE spectra of CuNCs (solid line) and Eu³⁺-CuNCs (dashed line). (C) Emission spectra of Eu³⁺-CuNCs. (D) PL decays of CuNCs (black curve) and Eu³⁺-CuNCs (red curve). Change of the PL intensity of CuNCs (black dots) and Eu³⁺-CuNCs (red dots) under (E) UV lamp and (F) daylight for different times.

As shown in Fig. 2A, UV-vis absorption peak of Eu³⁺-CuNCs shifted to 298 nm compared to the bare CuNCs (292 nm), which may be attributed to the increase in the particle size of CuNCs after doping with Eu³⁺ ion.¹⁹ Due to the small particle size of the nanoclusters themselves, the change of particle size of them could not be well distinguished by TEM images after doping with Eu³⁺ ion, thus, the diameter distribution (Fig. S3) was used to prove that the red shift of the UV-vis absorption band was caused by the increase of particle size after doping with Eu³⁺ ion. Comparing the PL behaviors of pure CuNCs and CuNCs in the Eu³⁺-CuNCs complex, Fig. 2B revealed that the shape of the photoluminescence excitation (PLE) spectra of Eu³⁺-CuNCs complex perfectly matched the one of CuNCs, indicating the doping of Eu³⁺ ion has no effect on the PL process of CuNCs. Fig. 2C showed the emission spectra of Eu³⁺-CuNCs, and an emission peak at 600 nm, while the respective PLE spectrum peaked at 395 nm. Meanwhile, PL decay curves of Eu³⁺-CuNCs also provided additional evidence for the incorporation of Eu³⁺ ion in NCs. As shown in Fig. 2D, average PL lifetime of CuNCs was 12.6 μs, which became shorter (11.0 μs) after doped Eu³⁺ ion, suggesting that energy transfer appeared from CuNCs to Eu³⁺ ion,²⁰ and the lifetime and proportion of each decay channel together with the calculated average lifetime are presented in Table S1. In order to further clarify the superiority of CuNCs after the doping of Eu³⁺ ion,

CuNCs and Eu^{3+} -CuNCs were consecutively exposed to UV irradiation and daylight for different times. Fig. 2E shows that the photostability of Eu^{3+} -CuNCs was indeed superior to pure CuNCs after exposure to sunlight for 12 h, as well as to UV irradiation for 2 h (Fig. 2F).

ECL-potential curves of bare glassy carbon electrode (GCE), and of the CuNCs- and Eu^{3+} -CuNCs-modified GCE (Fig. 3A) revealed the doping of Eu^{3+} ion caused a 3-fold enhancement in ECL intensity, which was mostly attributed to doping-induced improvement in the stability of reduced NCs. Moreover, the ECL intensity of CuNCs with different concentrations of Eu^{3+} ion doping was investigated (Fig. S4), and the optimal concentration ratio of Cu^{2+} to Eu^{3+} was found to be 4:1, possibly because NCs had the most homogeneous Eu^{3+} distribution under this doping level.^{2,18} Compared with the pure CuNCs/GCE in Fig. S5, the ECL signal of Eu^{3+} -CuNCs/GCE is more stable under 15 consecutive cyclic potential scans (Fig. 3B), which not only improved the ECL stability but enhanced the ECL intensity. As mentioned, ECL signal performance of Eu^{3+} -CuNCs was closely related to the stability of the reduced NCs, the inset of Fig. 3A displayed that the reduction peak and current of the co-reactant at Eu^{3+} ion doping was different from those of pure CuNCs due to the distinct surface states of NCs formed by doping with Eu^{3+} ion.² Besides, the ECL intensity was generated when the excited state returned to the ground state through radiative transition, it released additional energy in the form of photons, while energy also dissipated by other forms, such as internal conversion and intersystem crossing. This part of the dissipates energy cannot generate the ECL intensity, resulting in the ECL intensity of Eu^{3+} -CuNCs increased by 3-fold but the Eu^{3+} -doping caused at least a 5-fold enhancement in the reduction current. The possible synergistic effect between the NCs and rare earth element dopants was studied using the ECL spectrum. The ECL spectra of bare CuNCs and Eu^{3+} -CuNCs under a series of filters (400 - 700 nm) are displayed in Fig. S6. Bare CuNCs had only one wide peak at approximately 600 nm, which was attributed to recombination emission of surface states. The peak of Eu^{3+} -CuNCs at 460 nm could be attributed to the $7F_0 \rightarrow 5D_2$ transition of Eu^{3+} ion,^{10,21} the ECL emission of Eu^{3+} -CuNCs at 620 nm, which was attributed to recombination emission of surface states, was enhanced compared with that of pure CuNCs, and energy transfer between NCs and Eu^{3+} ion possibly resulted in the redshift of the emission peak.

Possible ECL mechanism of Eu^{3+} -CuNCs can be described as follows. First, Eu^{3+} -CuNCs obtained electrons to form Eu^{3+} -CuNCs* (eq. 1), and $\text{S}_2\text{O}_8^{2-}$, came from $\text{K}_2\text{S}_2\text{O}_8$ co-reactant, was reduced to $\text{SO}_4^{\bullet-}$ and SO_4^{2-} at the surface of the electrode (eq. 2), which was beneficial for enhancing the ECL signal. Then, Eu^{3+} -CuNCs* combined with $\text{SO}_4^{\bullet-}$ to generate Eu^{3+} -CuNCs* (eq. 3). Finally, the ECL signal was generated when Eu^{3+} -CuNCs* was converted into Eu^{3+} -CuNCs (eq. 4). The ECL signal can be effectively quenched by DA due to DA being oxidized by $\text{SO}_4^{\bullet-}$ and then generating the o-benzoquinone species (BQ). As shown in eq. 5, under this circumstance, the consumption of $\text{SO}_4^{\bullet-}$ leads to the decrease of Eu^{3+} -CuNCs* excited state (eq. 3

and 4), resulting in the ECL signal quenching.^{12,18,22} The reaction illustrating the ECL mechanism are as follows:

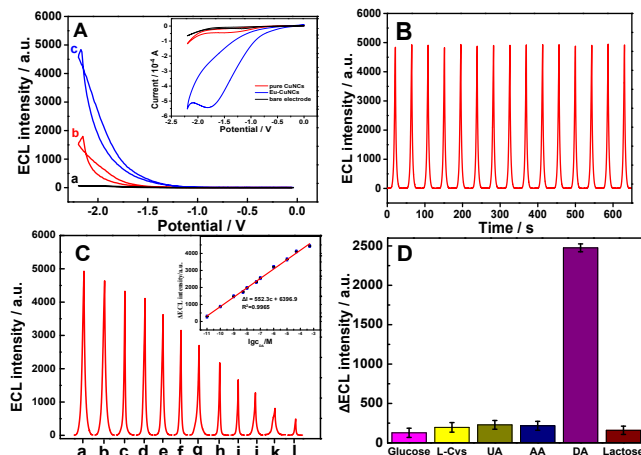
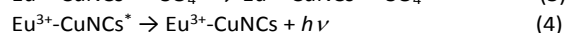
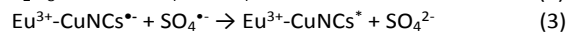


Fig. 3. (A) ECL-potential curves of bare GCE (a), pure CuNCs-modified GCE (b) and Eu^{3+} -CuNCs-modified GCE (c) under the potential scan of -2.2 to 0 V. Inset: corresponding cyclic voltammograms of bare GCE, pure CuNCs-modified GCE and Eu^{3+} -CuNCs-modified GCE. (B) The ECL stability of Eu^{3+} -CuNCs/GCE under 15 consecutive cyclic potential scans. (C) The signal response of the proposed ECL biosensor for detecting various concentrations of DA and corresponding concentrations of DA: 0, 1.0×10^{-11} M, 1.0×10^{-10} M, 1.0×10^{-9} M, 5.0×10^{-9} M, 1.0×10^{-8} M, 5.0×10^{-8} M, 1.0×10^{-7} M, 1.0×10^{-6} M, 1.0×10^{-5} M, 5.0×10^{-5} M, and 5.0×10^{-4} M (from a to l). Inset: linear relationship between the ΔECL intensity and the logarithm of DA concentrations. (D) Selectively of other interfering substances against 1.0×10^{-7} M DA: glucose, L-Cys, UA, AA, lactose (the concentration of the above interferents was 1.0×10^{-7} M of all). The above ECL signals were obtained in 0.1 M PBS (pH 7.4) containing 50 mM $\text{K}_2\text{S}_2\text{O}_8$ with 600 V PMT. The error bars represent the standard deviation of three repeated detections.

We have performed ECL measurements on Eu^{3+} -CuNCs/GCE electrodes at different concentrations of the analyte DA. As shown in Fig. 3C, the signal of ECL was quenched with the increasing concentration of DA, as described by the linear regression equation $\Delta I = 552.3 \lg C_{\text{DA}} + 6396.9$ ($R^2 = 0.9965$) ($\Delta I = I_0 - I$, I_0 and I represent ECL intensity without and with DA, and the logarithm of DA concentrations in the range from 1.0×10^{-11} to 5.0×10^{-4} M). Compared with the signal response of the pure CuNCs-modified GCE for detecting various concentrations of DA (Fig. S7), the doping of Eu^{3+} ion greatly improved the sensitivity of detecting DA. The minimum detection concentration of 1.0×10^{-11} M was used as the relative detection limit of the ECL biosensor based on Eu^{3+} -CuNCs/GCE for DA detection in this work, indicating that the

COMMUNICATION

Journal Name

proposed ECL biosensor is more sensitive than other ECL sensors (Table S2) and other methods for DA detection (Table S3).

The reproducibility of the proposed ECL biosensor was evaluated from the response to 1.0×10^{-7} M DA at five electrodes, and the relative standard deviation of the similar ECL responses between prepared electrodes was 5.4 % (Fig. S8), suggesting high reproducibility towards DA detection. Furthermore, the specificity of the proposed ECL biosensor for sensing DA was also investigated in this work. We measured several interfering substances, such as glucose, L-cysteine (L-Cys), uric acid (UA), ascorbic acid (AA), and lactose, with the same concentration of 1.0×10^{-7} M under the same experimental conditions. The obtained results are displayed in Fig. 3D. These small biomolecules had no obvious quenching effect on the ECL signal, which essentially suggests that the proposed biosensor had superior selectivity to identify the target and nontarget biomolecules.

In summary, Eu^{3+} -CuNCs were synthesized to solve the poor stability of CuNCs and low sensitivity of their ECL assays. Eu^{3+} ion alter the surfaces of CuNCs and drive the formation of new surface state ($\text{Eu}(\text{III})$ complex) to promote effective energy transfer from the host to the Eu^{3+} ion, resulting in greatly enhanced ECL emission intensity and stability of CuNCs. The as-synthesized Eu^{3+} -CuNCs were applied for the detection of DA, achieving a LOD of 1.0×10^{-11} M. In addition, the assay shows a strong selectivity to interfering substances. The presented results give us a clue to solve the stability issues of metal nanoclusters, provide a powerful tool for the developing ECL emitters, and may open the promising avenues to develop new ECL systems for medical and biological analysis.

The authors gratefully acknowledge the support of the National Natural Science Foundation of China (21778047, 21976209), the Hong Kong Scholars Program (XJ2017052), the Science Technology and Innovation Committee of Shenzhen Municipality (JCYJ20170818104224667) and Taishan Scholar Project Special Funding (No.ts20190962).

Conflicts of interest

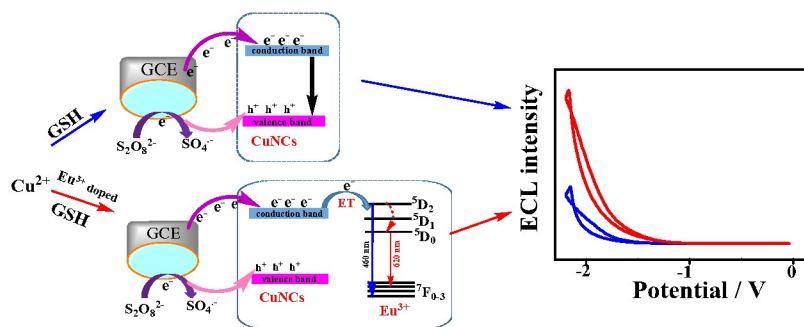
There are no conflicts to declare.

Notes and references

- (a) Y. J. Lin, P. C. Chen, Z. Yuan, J. Y. Ma and H. T. Chang, *Chem. Commun.*, 2015, **51**, 11983-11986; (b) X. F. Jia, J. Li, L. Han, J. T. Ren, X. Yang and E. K. Wang, *ACS Nano*, 2012, **6**, 3311-3317.
- (a) S. J. Payne, G. L. Fiore, C. L. Fraser and J. N. Demas, *Anal. Chem.*, 2010, **82**, 917-921; (b) L. Deng, Y. Shan, J.-J. Xu and H.-Y. Chen, *Nanoscale*, 2012, **4**, 831-836.
- L. F. Sun, L. Bao, B.-R. Hyun, A. C. Bartnik, Y.-W. Zhong, J. C. Reed, D.-W. Pang, H. D. Abruna, G. G. Malliaras and F. W. Wise, *Nano Lett.*, 2009, **9**, 789-793.
- (a) G. F. Jie, H. P. Huang, X. L. Sun and J.-J. Zhu, *Biosens. Bioelectron.*, 2008, **23**, 1896-1899; (b) Q. Liu, M. Han, J. C. Bao, X. Q. Jiang, Z. H. Dai, *Analyst*, 2011, **136**, 5197-5203.

- X. Y. Long, F. Zhang, Y. P. He, S. F. Hou, B. Zhang and G. Z. Zou, *Anal. Chem.*, 2018, **90**, 3563-3569.
- F. F. Jia, H. Zhong, W. G. Zhang, X. R. Li, G. Y. Wang, J. Song, Z. P. Cheng, J. Z. Yin, L. P. Guo, *Sensor. Actuat. B-Chem.*, 2015, **212**, 174-182.
- (a) L. Y. Chen, C. W. Wang, Z. Yuan and H. T. Chang, *Anal. Chem.*, 2014, **87**, 216-229; (b) X. F. Jia, X. Yang, J. Li, D. Li and E. K. Wang, *Chem. Commun.*, 2013, **50**, 227-229.
- H. P. Peng, M. L. Jian, Z. N. Huang, W. J. Wang, H. H. Deng, W. H. Wu, A. L. Liu, X. H. Xia and W. Chen, *Biosens. Bioelectron.*, 2018, **105**, 71-76.
- Y. Zhou, M. X. Chen, Y. Zhuo, Y. Q. Chai, W. J. Xu and R. Yuan, *Anal. Chem.*, 2017, **89**, 6787-6793.
- H. T. Liu, X. Q. Gao; X. M. Zhuang; C. Y. Tian; Z. G. Wang; Y. X. Li and A. L. Rogach, *Analyst*, 2019, **144**, 4425-4431.
- W.-F. Lai, W.-T. Wong and A. L. Rogach, *Adv. Mater.*, 2020, 1906872.
- M. Zhao, A. Y. Chen, D. Huang, Y. Zhuo, Y. Q. Chai and R. Yuan, *Anal. Chem.*, 2016, **88**, 11527-11532.
- (a) R. A. Wise, *Nat. Rev. Neurosci.*, 2004, **5**, 483-494; (b) Q. Lu, J. J. Zhang, X. F. Liu, Y. Y. Wu, R. Yuan and S. H. Chen, *Analyst*, 2014, **139**, 6556-62; (c) J. X. Li, X. J. Li, Y. H. Zhang, R. X. Li, D. Wu, B. Du, Y. Zhang, H. M. Ma and Q. Wei, *RSC Adv.*, 2015, **5**, 5432-5437.
- (a) F. D. P. Ferreira, L. I. B. Silva, A. C. Freitas, S. A. P. Rocha and A. C. Duarte, *J. Chromatogr. A*, 2009, **1216**, 7049-7054; (b) X. Zhang, X. Chen, S. Kai, H. Y. Wang, J. Yang, F. G. Wu and Z. Chen, *Anal. Chem.*, 2015, **87**, 3360-3365; (c) A. Abbaspour, A. Khajehzadeh and A. Ghaffarinejad, *Analyst*, 2009, **134**, 1692-1698; (d) X. M. Feng, C. J. Mao, G. Yang, W. H. Hou and J. J. Zhu, *Langmuir*, 2006, **22**, 4384-4389.
- (a) J. Wang, W. W. Zhao, X. R. Li, J. J. Xu and H. Y. Chen, *Chem. Commun.*, 2012, **48**, 6429-6431; (b) H. Zhou, J. Liu, J.-J. Xu and H.-Y. Chen, *Chem. Commun.*, 2011, **47**, 8358-8360; (c) M. M. Richter, *Chem. Rev.*, 2004, **104**, 3003-3036; (d) C. Y. Tian, L. Wang, F. Luan and X. M. Zhuang, *Talanta*, 2018, **191**, 103-108; (e) P. Bertocello and R. J. Forster, *Biosens. Bioelectron.*, 2009, **24**, 3191-3200.
- Z. G. Wang, A. S. Susha, B. K. Chen, C. Reckmeier, O. Tomanec, R. Zboril, H. Z. Zhong and A. L. Rogach, *Nanoscale*, 2016, **8**, 7197-7202.
- (a) X. F. Wang, J.-J. Xu and H.-Y. Chen, *J. Phys. Chem. C*, 2008, **112**, 17581-17585; (b) Y. Shan, J.-J. Xu and H.-Y. Chen, *Chem. Commun.*, 2009, **28**, 905-907.
- Q. Liu, X. P. Liu, Y. P. Wei, C. J. Mao, H. L. Niu, J. M. Song, B. K. Jin and S. Y. Zhang, *Microchim Acta*, 2017, **184**, 1353-1360.
- (a) Z. Fang, L. Liu, L. L. Xu, X. G. Yin and X. H. Zhong, *Nanotechnology*, 2008, **19**, 235603; (b) K. X. Zhang, R. Zhang, Y. X. Yu and S. Q. Sun, *J. Nanosci. Nanotechnol.*, 2012, **12**, 3011-3017; (3) K. X. Zhang, Y. X. Yu and S. Q. Sun, *Appl. Surf. Sci.*, 2012, **258**, 7658-7663.
- (a) G. X. Jiang, A. S. Susha, A. A. Lutich, F. D. Stefani, J. Feldmann and A. L. Rogach, *ACS Nano*, 2009, **3**, 4127-4131; (b) Y. L. He, J. L. He, H. R. Zhang, Y. L. Liu, B. F. Lei, *J. Colloid Interf. Sci.*, 2017, **496**, 8-15.
- (a) S. Sarkar, M. Chatti, and V. Mahalingam, *Chem. Eur. J.*, 2014, **20**, 3311-3316; (b) K. Naveen Kumar, K. Sivaiah and S. Buddhudu, *J. Lumin.*, 2014, **147**, 316-323.
- X. Liu, H. Jiang, J. P. Lei and H. X. Ju, *Anal. Chem.*, 2007, **79**, 8055-8060.

A graphical and textual abstract for the *Table of contents entry*



We reported an electrochemiluminescence biosensing platform based on europium(III)-doped copper nanoclusters that exhibited excellent analytical performances of highly stability and enhanced intensity.